Three-dimensional band structure and bandlike mobility in oligoacene single crystals: A theoretical investigation

Y. C. Cheng, R. J. Silbey, D. A. da Silva Filho, J. P. Calbert, J. Cornil et al.

Citation: J. Chem. Phys. **118**, 3764 (2003); doi: 10.1063/1.1539090
View online: http://dx.doi.org/10.1063/1.1539090
View Table of Contents: http://jcp.aip.org/resource/1/JCPSA6/v118/i8
Published by the American Institute of Physics.

Three-dimensional band structure and bandlike mobility in oligoacene single crystals: A theoretical investigation

Y. C. Cheng[a] and R. J. Silbey[b]
Department of Chemistry and Center for Materials Science and Engineering, Massachusetts Institute of Technology, Cambridge, Massachusetts 02139

D. A. da Silva Filho, J. P. Calbert,[c] J. Cornil,[c] and J. L. Brédas
Department of Chemistry, The University of Arizona, Tucson, Arizona 85721-0041

(Received 30 August 2002; accepted 25 November 2002)

Quantum-chemical calculations coupled with a tight binding band model are used to study the charge carrier mobilities in oligoacene crystals. The transfer integrals for all nonzero interactions in four crystalline oligoacenes (naphthalene, anthracene, tetracene, and pentacene) were calculated, and then used to construct the excess electron and hole band structures of all four oligoacene crystals in the tight binding approximation. From these band structures, thermal-averaged velocity–velocity tensors in the constant-free-time and the constant-free-path approximations for all four materials were calculated at temperatures ranging from 2 to 500 K. The bandwidths for these oligoacenes were found to be of the order of 0.1–0.5 eV. Furthermore, comparison of the thermal-averaged velocity–velocity tensors with the experimental mobility data indicates that the simple band model is applicable for temperatures only up to about 150 K. A small-polaron band model is also considered, but the exponential band narrowing effect is found to be incompatible to experimental power law results. © *2003 American Institute of Physics.*
[DOI: 10.1063/1.1539090]

I. INTRODUCTION

The study of charge-carrier mobilities in organic molecular crystals has continued for more than 30 years,[1,2] but the problem of the best way to describe the motion of charge carriers in the crystal has still not been fully resolved.[3,4] Recently, the realization of electronic devices based on crystalline organic materials has renewed the interest in developing new theoretical models to better understand this problem,[5–7] and new techniques developed for preparing ultrapure single crystals of these organic materials have enabled the study of intrinsic charge transport mechanisms.[8–11] Because the mobility is an important factor for potential electronic applications, it is of importance that we develop a theoretical model capable of describing the charge transport mechanism in organic molecular crystals.

The measured intrinsic mobilities of oligoacene single crystals show a band to hopping transition occurs at about room temperature,[4,12,13] which enables us to characterize the charge-transport mechanism in two different regimes, bandlike mechanism at low temperature, and hopping mechanism at high temperature. Although that this transition occurs because of the effect of electron–phonon coupling is widely accepted, a quantitative theory that can describe the charge-carrier behavior in both regimes is still missing, especially for the wider band materials, tetracene and pentacene. The polaron model has been applied to earlier studies on naphthalene with some success.[12,14–16]

The charge transport in the bandlike regime of oligoacene crystals is of particular interest, because relatively high charge carrier mobilities, ranging from 1 to 10 $cm^2/V\,s$ at room temperature to more than 10^2 $cm^2/V\,s$ at low temperature, have been achieved in well ordered materials.[6,8,10,17] In addition, the measured mobilities follow the power law temperature dependence $\mu \sim T^{-n}$ with $n \approx 1.5-3.0$ in the bandlike regime. This power law dependence suggests a wide-band theory may be applicable in highly purified aromatic molecular single crystals, but so far all theoretical calculations have failed to provide the correct magnitudes and temperature dependences of the charge-carrier mobilities in organic molecular crystal systems.[4,18,19] Karl *et al.* have used a standard wide-band theory to describe the high, field-dependent hole mobilities observed in naphthalene at low temperature, and obtained a reasonable fit to their field-dependent results.[8] They concluded that a classical band-type transport model with combined acoustic- and optical-phonon scattering in nonparabolic bands is suitable for describing the mobilities in naphthalene at low temperature. However, because of the lack of reliable information on the band structure of the system, an important problem about the consistency of the band picture was left unanswered in their paper. Due to the advances of modern quantum-chemical techniques, it is now possible to compute the band structure and examine the wide-band model theoretically. Therefore, an investigation based on purely theoretical parameters and modeling is essential to interpret new experimental developments and better understand the underlying transport mechanism.

In this paper, a band model coupled with quantum-chemistry calculations is used to study the charge carrier

[a]Electronic mail: yccheng@mit.edu
[b]Electronic mail: silbey@mit.edu
[c]Permanent address: Center for Research in Molecular Electronics and Phontonics, University of Mons-Hainaut, B-7000 Mons, Belgium.

mobilities in oligoacene crystals. Recently, Cornil *et al.* have developed a semiempirical Hartree–Fock intermediate neglect of differential overlap (INDO) method which can be used to obtain good estimates of the transfer integrals in van der Waals bonded crystals.[20–22] Here we adopt this method to calculate transfer integrals for all nonzero interactions in naphthalene, anthracene, tetracene, and pentacene crystals, and then use these parameters to obtain the band structures and the mobility tensors for these crystals. A tight binding method first proposed by LeBlanc[2] and then extended by Katz *et al.*[23] in the early 1960s is used to construct the band structure, and the velocity–velocity tensor products are averaged over the Boltzmann distribution among the energy bands. In addition, in order to account for the effect of electron–phonon coupling under the framework of a basic band model, we discuss the polaron band theory and its applicability. Throughout this work, we focus on the behavior of charge carriers in the low temperature bandlike regime, and neglect the hopping regime. The goal of this investigation is to re-examine the standard wide-band description of the mobility in oligoacene compounds based on the new parameters, and provide information about the applicability of the simple wide-band model.

II. METHOD

A. Theoretical background

The model adopted here for calculating the band structure and the mobility tensors for organic molecular crystals was first proposed by LeBlanc[2] and then extended by Katz *et al.*[23] in the early 1960s. Note that since all the compounds investigated here have a crystal structure containing two molecules (say, type α and type β) in a unit cell, there are two bands arising from the symmetric and antisymmetric combinations of molecular wave functions in a cell for both excess-electron and excess-hole. Assuming the concentration of charge carriers is very small so that one-particle formalism is applicable, and the excess electron or hole does not significantly change the wave function of the molecule, the lowest unoccupied molecular orbital (LUMO) of a molecule can be used as a basis for crystal electron wave functions, and the highest occupied orbital (HOMO) can be used for hole wave functions. In the tight binding approximation, the energies of the two excess-electron (excess-hole) bands, $E_+(\mathbf{k})$ and $E_-(\mathbf{k})$, can be expressed in terms of the transfer integrals between molecular LUMOs (HOMOs),[23]

$$E_\pm(\mathbf{k})=\left(\frac{T_\alpha+T_\beta}{2}\right)\pm\sqrt{\left(\frac{T_\alpha-T_\beta}{2}\right)^2+V(\mathbf{k})^2}. \tag{1}$$

For crystals with inversion symmetry,

$$T_\alpha=E_\alpha-2\cdot\sum_i t_i^\alpha\cdot\cos(\mathbf{k}\cdot\mathbf{r}_i^\alpha), \tag{2}$$

$$T_\beta=E_\beta-2\cdot\sum_i t_i^\beta\cdot\cos(\mathbf{k}\cdot\mathbf{r}_i^\beta), \tag{3}$$

$$V(\mathbf{k})=-2\cdot\sum_i t_i^{\alpha\beta}\cdot\cos(\mathbf{k}\cdot\mathbf{r}_i^{\alpha\beta}), \tag{4}$$

where $\mathbf{k}$ is the wave vector; T_α and T_β represent the interactions between *translationally equivalent* molecules, E_α and E_β are the corresponding molecular orbital energy on monomer-type α and β, respectively; the summation in T_α (T_β) is taken over all interacting *translationally equivalent* molecules; t_i^α (t_i^β) is the intermolecular transfer integral between the central type α (β) molecule and the type α (β) molecule at the ith unit cell. For crystals with a unit cell containing two equivalent molecules, $E_\alpha=E_\beta$ and $t_i^\alpha=t_i^\beta$; $\mathbf{r}_i^\alpha$ ($\mathbf{r}_i^\beta$) is the vector from the center type $\alpha(\beta)$ molecule to the type $\alpha(\beta)$ molecule at the ith unit cell; $V(\mathbf{k})$ represents the interaction between type α and β molecules, and the summation is over all interacting *translationally inequivalent* molecules; $t_i^{\alpha\beta}$ is the intermolecular transfer integral between the central molecule and the *translationally inequivalent* molecule at the ith unit cell, and $\mathbf{r}_i^{\alpha\beta}$ is the vector connecting these two molecules.

Equations (1)–(4) are the necessary analytical equations for constructing the energy band structure for an excess electron or an excess hole in a crystal with two molecules in a unit cell, regardless of the details of crystal structure and intermolecular interactions. In addition, the velocity of charge carriers can be calculated from the band structure. In a standard band-theory model, the group velocity $\mathbf{v}$(k) of the delocalized electron waves or hole waves is given by the gradient of the band energy in k-space,

$$\mathbf{v}(\mathbf{k})=(1/\hbar)\cdot\nabla_k E(\mathbf{k}). \tag{5}$$

Although it is not possible to directly calculate the value of the mobility tensor using a band model, we can use two simplified models for the relaxation time to evaluate important parameters related to the mobility tensors.[2,23,24] Given a constant isotropic relaxation time τ_0 (constant-free-time approximation) or a constant isotropic free path λ (constant-free-path) for the motion of the charge carriers in the crystal, the components of the mobility tensor are

$$\mu_{ij}=e\tau_0\langle v_i v_j\rangle/kT, \tag{6}$$

and

$$\mu_{ij}=(e\lambda/kT)\langle v_i v_j/|\mathbf{v}(\mathbf{k})|\rangle, \tag{7}$$

in the constant-free-time and constant-free-path approximations, respectively. Here v_i is the ith component of the group velocity, $\mathbf{v}(\mathbf{k})$, and the bracket in the equation means an average over the Boltzmann distribution of a charge carrier in the energy bands,

$$\langle v_i v_j\rangle=\frac{\int\left\{\frac{\partial E_+}{\partial k_i}\frac{\partial E_+}{\partial k_j}e^{-\beta E_+(\mathbf{k})}+\frac{\partial E_-}{\partial k_i}\frac{\partial E_-}{\partial k_j}e^{-\beta E_-(\mathbf{k})}\right\}d\mathbf{k}}{\hbar^2\int\{e^{-\beta E_+(\mathbf{k})}+e^{-\beta E_-(\mathbf{k})}\}d\mathbf{k}}, \tag{8}$$

where $E_+(\mathbf{k})$ is the energy of the upper band, and $E_-(\mathbf{k})$ is the energy of the lower band, as described in Eq. (1). Integrals in Eq. (8) can be evaluated numerically to obtain the values of thermal-averaged velocity–velocity tensor products $\langle v_i v_j\rangle$ and $\langle v_i v_j/|\mathbf{v}(\mathbf{k})|\rangle$. The two terms, $\langle v_i v_j\rangle$ and $\langle v_i v_j/|\mathbf{v}(\mathbf{k})|\rangle$, are the main quantities of concern here, for

TABLE I. Crystal constants and structures of oligoacenes.

Crystal constants	Naphthalene Monoclinic	Anthracene Monoclinic	Tetracene Triclinic	Pentacene Triclinic
a[a]	8.0980	8.4144	6.057	6.275
b	5.9530	5.9903	7.838	7.714
c	8.6520	11.0953	13.010	14.442
α[b]	90.000	90.000	77.13	76.75
β	124.400	125.293	72.12	88.01
γ	90.000	90.000	85.79	84.52

[a]Units in Å.
[b]Units in deg.

they can serve as estimates of the values of the real mobility tensors under the constant-free-time or constant-free-path approximations.

B. Numerical calculations

Values of important parameters in the band equations [Eqs. (1)–(4)] can be evaluated using numerical methods. In this investigation, the values of site energy and transfer integrals were calculated using the INDO semiempirical quantum-chemical method.[21,22,25] Using crystal structures taken from the Cambridge database, parameters for four crystalline oligoacenes (naphthalene,[26] anthracene,[27] tetracene, and pentacene)[28] were calculated by performing ZINDO (Refs. 20 and 29) calculations on all molecular dimers within the third nearest-neighbor shells for each crystal. The crystal data used in our calculations are listed in Table I. Because it is highly unlikely that molecules located outside the third shell will interact with the central molecule, we expect that all nonzero interactions are included in our calculations. Note that special attention needs to be paid to the phase of the macromolecule wave functions to determine the correct signs of the transfer integrals. Once we have the site energy and transfer integrals, analytical expressions of the energy bands as a function of the wave vector, k, can be obtained using Eqs. (1)–(4). In addition, the 3D total density of states (DOS) can be calculated by performing a primitive histogram calculation inside the first Brillouin zone.

Because the unit cell vectors **a**, **b**, and **c** are not orthogonal to each other for the crystals investigated here, a new Cartesian coordinate system was used to perform the group velocity calculations. The new coordinate system is chosen as follows: the new x-axis is parallel to the **a** direction, the y-axis is on the **ab** plane and points to the positive **b** direction, and the new z-axis is parallel to the interlayer $\mathbf{c}'$ direction which is perpendicular to the **ab** plane. The group velocity of charge carriers in the energy band was calculated according to Eq. (5) in the new coordinate system, and projected back to each unit cell direction to evaluate the velocity vector in the real space. The thermal-averaged integral [Eq. (8)] was evaluated by applying an adaptive Gaussian integration method using a 51-point Gauss–Kronrod rule over the first Brillouin zone with more than $102\times102\times102$ points. The estimated absolute error is $<10^{-6}$ in all numerical integrations performed. Values of the thermal-averaged velocity–velocity tensor products were calculated at temperatures ranging from 1.7 K to 500 K.

III. RESULTS AND DISCUSSION

A. Transfer integrals

The calculated site energies and transfer integrals for all four oligoacenes are listed in Table II. The calculated site energies for type α and type β molecules in naphthalene and anthracene crystals are the same because of their monoclinic

TABLE II. Calculated site energy and transfer integrals (units: meV).

			Naphthalene		Anthracene		Tetracene		Pentacene	
			HOMO	LUMO	HOMO	LUMO	HOMO	LUMO	HOMO	LUMO
	ΔE[a]		0	0	0	0	48	−52	0.0	−2
a[b]	b	c								
1	0	0	0.00	0.00	0.00	0.00	−29.25	33.33	49.93	48.30
0	1	0	38.50	11.15	48.30	29.93	0.00	0.00	0.00	0.00
−1/2	1/2	0	36.59	−41.49	−47.89	−56.05	−68.88	−70.80	−97.82	−81.08
1/2	1/2	0	36.59	−41.49	−47.89	−56.05	−61.92	−47.42	−72.65	−81.62
−3/2	1/2	0	0.00	0.00	0.00	0.00	0.00	15.88	−4.61	−5.74
3/2	1/2	0	0.00	0.00	0.00	0.00	−14.56	0.0	−4.75	−3.22
−1/2	3/2	0	−2.99	−2.99	−3.40	−3.26	0.00	0.00	0.00	0.00
1/2	3/2	0	−2.99	−2.99	−3.40	−3.26	0.00	0.00	0.00	0.00
0	−1	1	−1.49	−4.08	0.0	−2.31	1.08	−3.53	3.12	0.0
1/2	1/2	1	−13.60	−4.21	−13.87	−3.80	0.00	0.00	0.00	0.00
1/2	−1/2	1	−13.60	−4.21	−13.74	−3.80	6.82	0.00	−2.43	0.00
−1/2	−1/2	1	0.00	0.00	0.00	0.00	−12.63	0.0	−2.29	−5.33
−1/2	−3/2	1	0.00	0.00	0.00	0.00	0.00	−7.58	0.00	−1.21
1/2	−3/2	1	−1.22	1.08	1.22	−1.22	0.00	0.00	0.00	−2.04
1/2	3/2	1	−1.22	1.08	1.22	−1.22	0.00	0.00	0.00	0.00
−3/2	−1/2	1	0.00	0.00	0.00	0.00	0.00	−9.33	0.0	−1.72
3/2	−1/2	1	1.63	1.63	1.63	1.49	0.00	0.00	0.00	0.00
3/2	3/2	1	1.63	1.63	1.63	1.49	0.00	0.00	0.00	0.00
−3/2	−3/2	1	0.00	0.00	0.00	0.00	−5.13	0.00	0.00	0.00

[a]Relative on-site energy, $E_\beta - E_\alpha$.
[b]Unit vectors being the lattice vectors.

$\mathbf{P}2_1/a$ symmetry. However, in tetracene and pentacene crystals, which have a triclinic $\mathbf{P}\bar{1}$ symmetry, an energy difference is found between type α and type β molecules. This energy difference is due to a slight geometry difference between type α and type β molecules, and leads to a significant difference in the band structures, as we will see in the next section.

For all compounds investigated here, calculated intralayer interactions are significantly larger than interlayer interactions. The important in-plane interactions found are those along the nearest-neighbor directions, d_1 (1/2, 1/2, and 0 along the *a*, *b*, and *c* directions) and d_2 ($-1/2$, 1/2, and 0 along the *a*, *b*, and *c* directions), and short crystal axis (*b* for naphthalene and anthracene, *a* for tetracene and pentacene); these results are in agreement with previous calculations for oligoacene crystals[22,24,30] and mobility measurements pointing to two-dimensional transport in oligoacene crystals.[11,31,32]

The evolution of the size of transfer integrals with respect to the size of oligoacene molecules, from two rings in naphthalene to five rings in pentacene, indicates that the size of the conjugated π system and the structure of the crystal are both important factors determining the strength of the interactions.[33] We find that as the size of the molecule increases, the calculated interactions for both holes and electrons along d_1 and d_2 increase; this contrasts with the situation observed in cofacial dimers (where the HOMO splitting decrease with increasing chain size), thus pointing to the subtle interplay between crystal packing and calculated transfer integrals.[33] Interestingly, interactions between molecules located in adjacent layers (along the *c* direction) decrease as the size of the molecule increases. This result can be attributed to the longer distance between layers in larger molecules. As the distances between the adjacent layers increase, the weak $\pi-\pi$ interactions along the *c* direction decrease.

B. Band structure and density of states

The DOS spectra and band structures along different unit cell vectors are displayed in Figs. 1–4 for naphthalene, anthracene, tetracene, and pentacene, respectively. Shapes of LUMO and HOMO bands along the k_a, k_b, k_c, k_{d1}, and k_{d2} directions are plotted. Note that the values of the *k* vectors are scaled such that the value at the first Brillouin zone edge is unity. The band structures of tetracene and pentacene are slightly different from those of naphthalene and anthracene, which can be ascribed to the different crystal structures and the significant energy differences between type α and type β molecules in the tetracene crystal. For monoclinic naphthalene and anthracene crystals, the degeneracy at the Brillouin zone edge on the **ab** plane due to the crystal glide plane symmetry can be clearly seen in the graph, as well as the Van Hove singularities around the band edges. Because no such symmetry exists in triclinic crystals, there is no degeneracy at the zone edge in the results for tetracene and pentacene crystals. The largest contribution to the energy splitting at the zone edge is from the difference between $\alpha-\beta$ site energies, so that the size of the splitting is approximately twice the size of the site energy difference. In all cases, the dispersion along the *c* direction is much smaller than those along the other directions, and a large gap is found between upper and lower bands along the *c* direction. This is clearly due to smaller interactions between molecules located in adjacent layers, and is a well known result for this kind of herringbone packing material.[22–24] As a result, we expect the charge carrier mobilities along the *c* direction to be smaller than those along other directions,

The bandwidth values for all oligoacenes are summarized in Table III. Bandwidths along the **a**, **b**, **c**, $\mathbf{d}_1$, $\mathbf{d}_2$ directions and the 3D total bandwidths calculated from the widths of the continuous region in the DOS spectrum are listed in Table III, as well as values of the gaps between the upper and lower bands in each direction. All four compounds investigated here have a continuous band with widths from 400 meV to 700 meV, in agreement with recent experimental and theoretical results.[8,11,22,34] In addition, comparing the total bandwidth for different oligoacenes, we find that the bandwidth increases when the size of the molecule increases, as we expect for herringbone structures.[33]

When the thermal populations of the charge carriers are taken into account, a parameter other than total bandwidth should be adopted for comparing intrinsic transport properties. For all the compounds investigated here, the bandwidths are significantly larger than the thermal energy, i.e., $W \gg kT$. This result implies that a wide band limit can be used to describe the transport of excess holes or excess electrons, and at normal temperatures, only the states around the energy minima of the band are populated. Note that due to the nature of the excess charge carriers, the energy of an excess electron is measured upward from the bottom of the lower band, while the energy of an excess hole is measured downward from the top of the upper band. That is, within this two-band model, the motion of the excess electrons in the crystal are governed by the lower LUMO band, while the motion of the excess holes are governed by the upper HOMO band.

Previous theoretical investigations have often used total bandwidths as criteria for comparing intrinsic excess electron and excess hole mobilities, but comparing values of total bandwidths can be misleading. For example, in a pentacene crystal, the total bandwidths of HOMO and LUMO bands along the d_1 direction (which is the direction with the strongest interaction) are approximately the same (738 meV and 728 meV, respectively); this could easily lead to the conclusion that the electrons can be as mobile as holes in pentacene crystals. However, if we consider the thermal population and compare mobilities according to the width of the upper HOMO band for excess hole and the lower LUMO band for excess electron (523 meV and 183 meV, respectively), the intrinsic excess hole mobility is predicted to be significantly larger than the intrinsic excess electron mobility in a pentacene crystal. Therefore, the width of the upper HOMO band appears to be a better parameter for estimating excess hole mobility, and the width of the lower LUMO band is a better parameter for estimating excess electron mobility. According to these two criteria, we predict all oligoacenes investigated

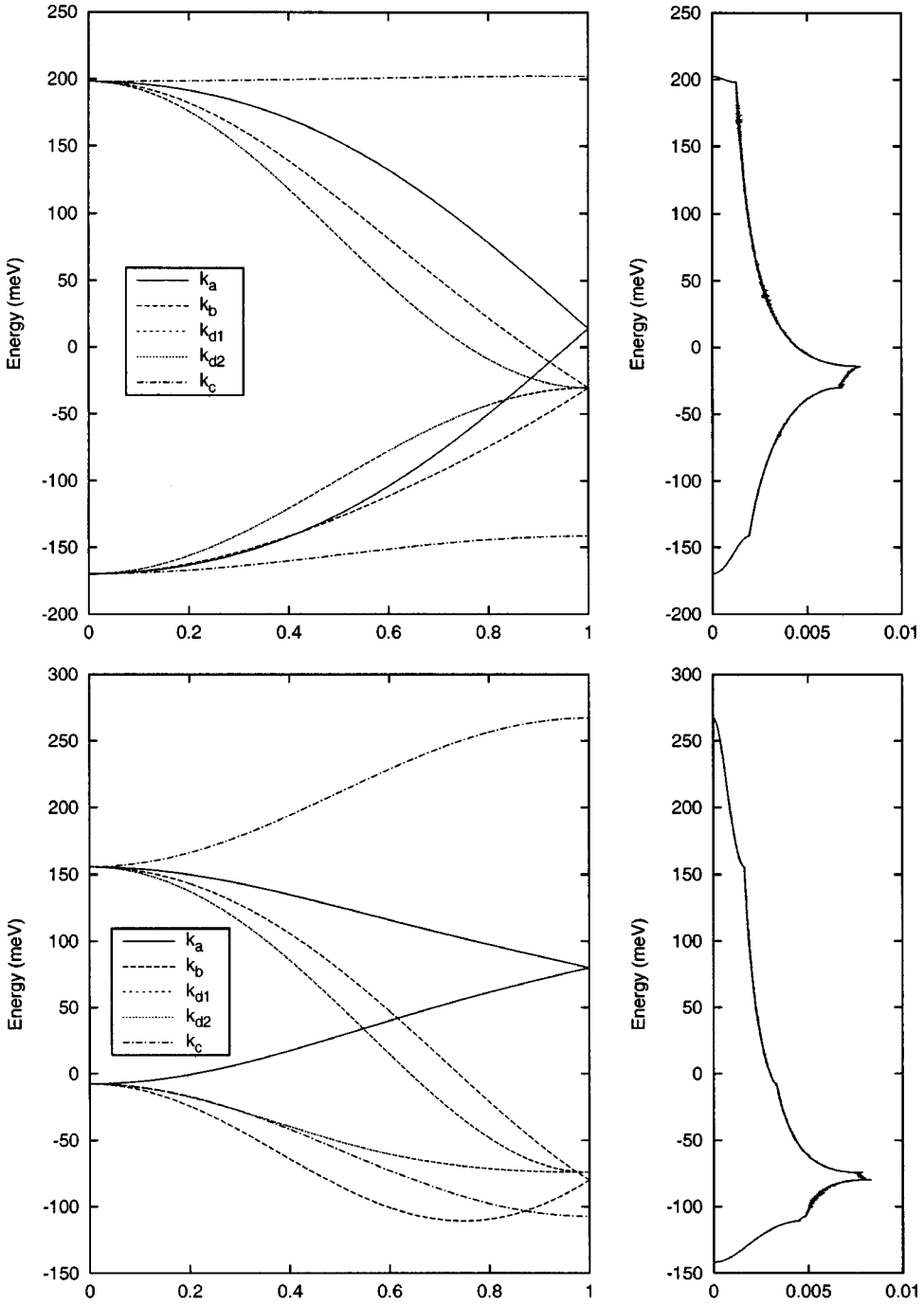

FIG. 1. Shape of the LUMO band (upper panel) and the HOMO band (lower panel) of naphthalene in the major crystal directions; the right panel is the corresponding density of states.

here to have higher excess hole mobilities, in agreement with experimental results.[11,31]

C. Thermal averaged velocity–velocity tensor

The calculated thermal-averaged velocity–velocity tensor products in constant-free-time and constant-free-path approximations for naphthalene in the temperature range from 1.7 K to 300 K are presented in Fig. 5. Data for all other oligoacene crystals have a similar temperature dependence and are therefore not presented here. For all four crystals studied here, the components $\langle V_a V_a \rangle$ and $\langle V_b V_b \rangle$ show a linear temperature dependence at temperatures higher than 10 K, which can be ascribed to the increasing thermal population of higher energy states. The component $\langle V_{c'} V_{c'} \rangle$ behaves differently and saturates quickly at about 100 K, which can be easily understood by considering the small bandwidth ($\sim$30 meV) and the band gap along the $\mathbf{c}'$ direction. Because of the small bandwidth along this direction, charge carriers quickly populate the nonparabolic part of the band as temperature increases, resulting in the saturation of the group velocity of charge carriers. To test the result, we calculated values of the other two diagonal components at higher temperatures, no saturation behavior can be observed in $\langle V_a V_a \rangle$ and $\langle V_b V_b \rangle$ up to 1000 K, in agreement with the larger values of bandwidths along these directions.

The amplitude of $\langle V_{c'} V_{c'} \rangle$ at low temperatures is comparable to or even larger than the components along the **a** and **b** directions. This result seems to be contrary to the

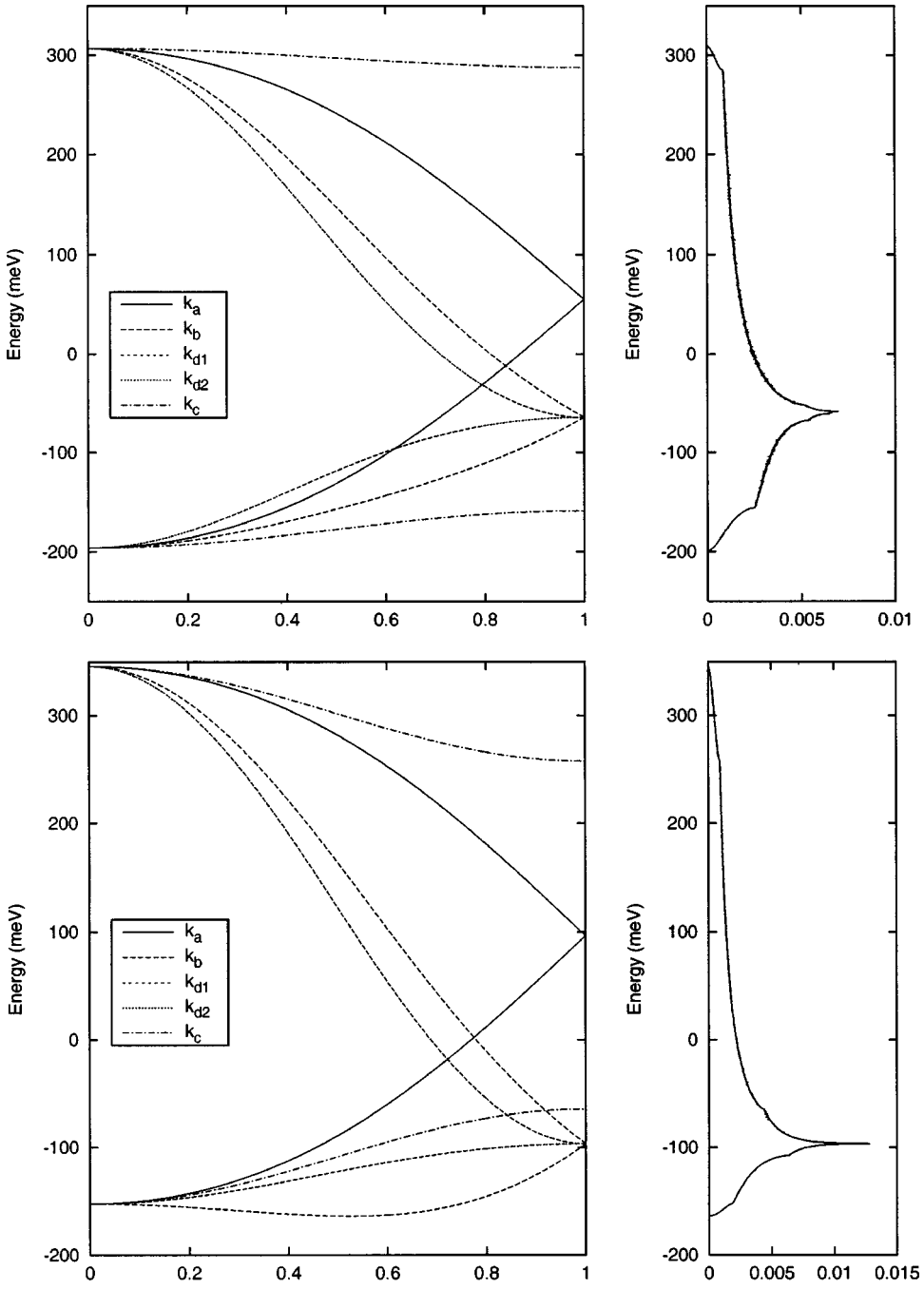

FIG. 2. Shape of the LUMO band (upper panel) and the HOMO band (lower panel) of anthracene in the major crystal directions; the right panel is the corresponding density of states.

general belief that the in-plane mobilities are significant higher than the perpendicular ones in oligoacene single crystals, and the result that the transfer integral along the $\mathbf{c}'$ direction is much smaller than transfer integrals on the plane. However, on closer inspection, the unexpected large value of $\langle V_{c'} V_{c'} \rangle$ can be explained by considering the thermal population of the electronic states. The states at the bottom of the band have zero velocities. Therefore, in order to obtain any nonzero velocity, states with higher energy have to be populated. If the band is narrow, states with higher velocity can be populated at lower temperature; if the band is broad, then only states with low velocity are populated at low temperature. As a result, the value of $\langle V^2 \rangle$ is a trade-off between the width of the band and the population of states with higher velocity (which is easier to achieve for narrower bands).

Table IV lists values of six tensor components for all four oligoacene crystals at 50 K. Note that for crystals with monoclinic unit cells, such as naphthalene and anthracene, the **b** direction is one of the three principal axes, so that there are only four nonzero mobility components. However, the orientations of the three principal axes for the triclinic unit cells are not unique, and in general all six mobility tensor components for tetracene and pentacene crystals are nonzero. Given the approximations in our model, these velocity–velocity tensor products contain the contribution to the charge carrier mobility from the potential energy field applied to the charge carrier. Therefore, diagonal components of these products can be seen as the theoretical upper bound of the charge carrier mobilities when scattering processes are omitted. Values of these tensor components again suggest

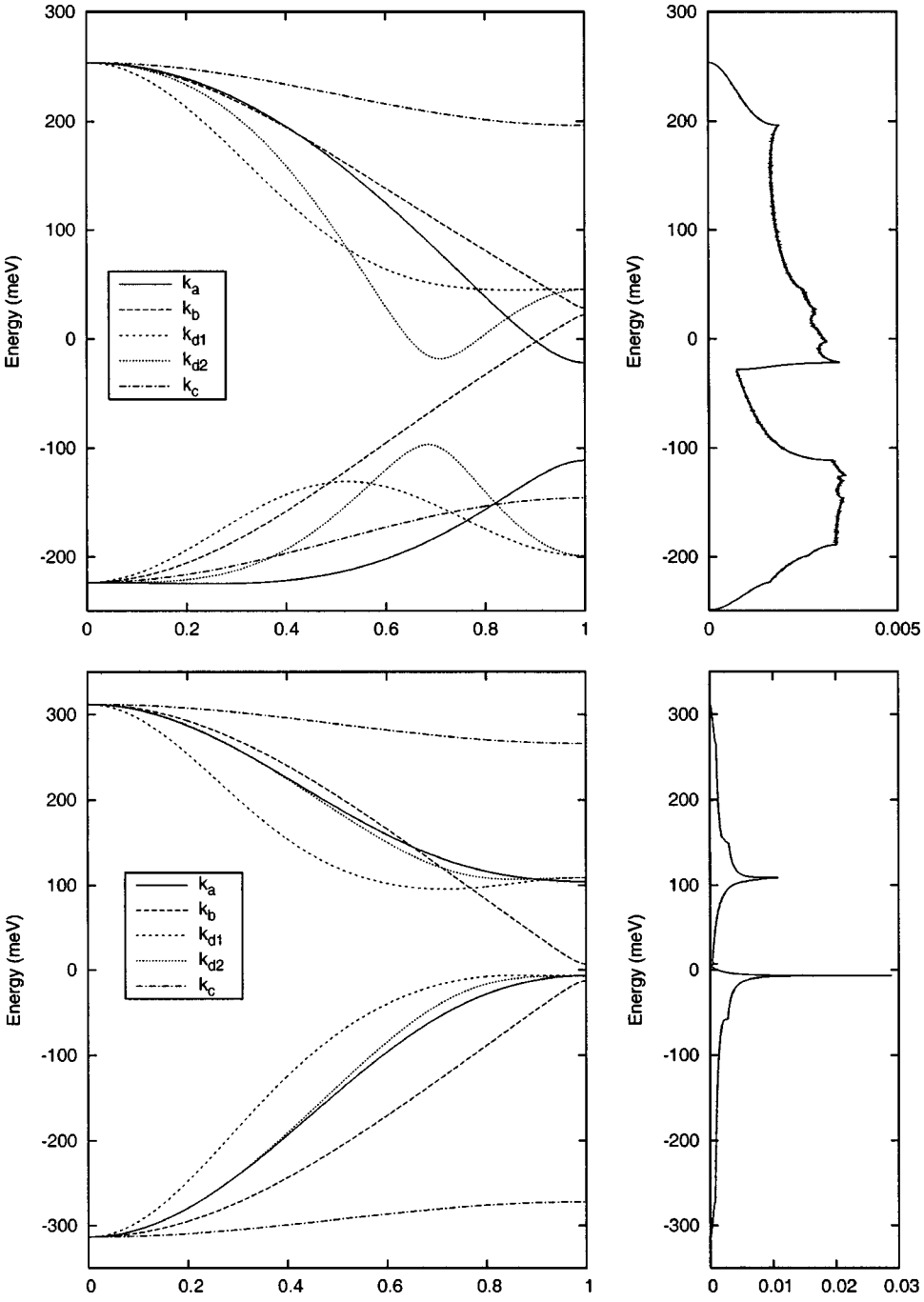

FIG. 3. Shape of the LUMO band (upper panel) and the HOMO band (lower panel) of tetracene in the major crystal directions; the right panel is the corresponding density of states.

that the excess hole mobility is higher than the excess electron mobility in oligoacene crystals, and that the mobilities increase with chain length in agreement with the previous considerations. Furthermore, great variations between values of components along different directions indicate highly anisotropic crystal environments in these crystals.

D. Self-consistency check on the band model

The use of a band representation to describe the motion of the charge carriers in the crystal can be justified only when both the mean free path exceeds many intermolecular distances and the uncertainty in the energy of the scattered carriers does not exceed the bandwidth,

$$\lambda \gg a_0,$$

$$W \gg \hbar/\tau_0.$$

For the crystals studied here $a_0 \approx 5$ Å and $W \approx 0.5$ eV, therefore the criteria for band theory to be applicable are λ longer than 5 Å and τ_0 larger than 10^{-15} s. To examine the applicability of the band model used in our calculations, the temperature dependent mean free time and mean free path were calculated by fitting the available experimental mobility data[11,18] to our theoretical thermal-averaged velocity-velocity tensor products using Eqs. (6) and (7). The results in the temperature range from 30 K to 300 K for excess hole in naphthalene crystal are presented in Fig. 6.

From Fig. 6, it can be clearly seen that the above criteria are fulfilled only at a temperature lower than 150 K, and any application of this simple band model to temperatures higher

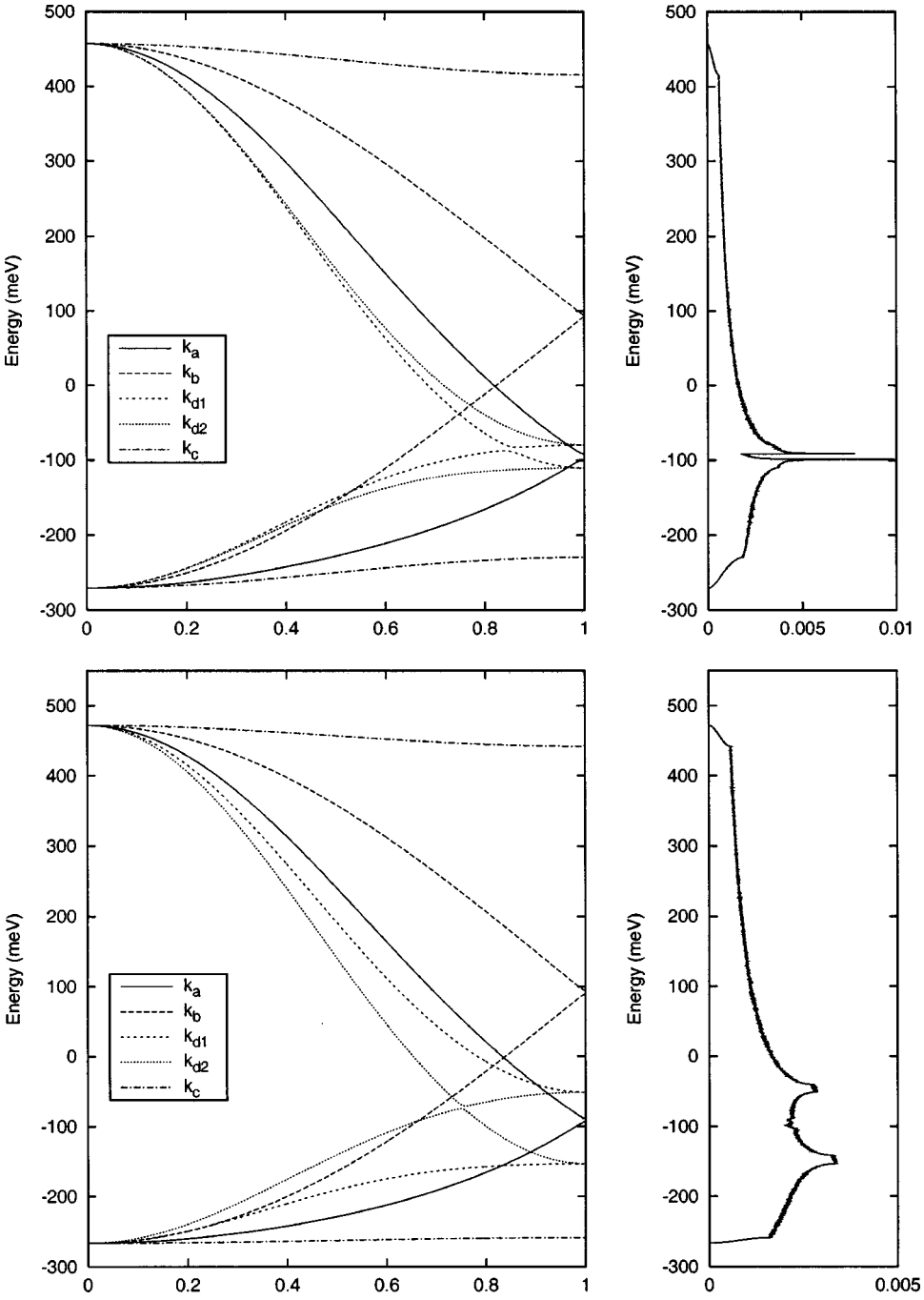

FIG. 4. Shape of the LUMO band (upper panel) and the HOMO band (lower panel) of pentacene in the major crystal directions; the right panel is the corresponding density of states.

than 150 K is open to criticism. In addition, the calculated results along different directions are significantly different, which implies that the scattering processes are highly anisotropic.

Because of possible highly anisotropic scattering processes, the use of constant-free-path or constant-free-time approximations should be treated with care, and a better approach would be to consider the free time or free path as a temperature dependent tensor property of the crystal. Basically, the present model keeps the mobility anisotropy originating from the energy band structure in the averaged velocity–velocity tensor, and puts dynamic effects related to the scattering processes into the constant-free-path or constant-free-time terms. Using only averaged free time or free path to describe the scattering processes can only be justified when the following conditions are all fulfilled: (i) The scattering processes along the three different crystal directions are the same; (ii) coupling between charge carriers and crystal phonons is small; (iii) molecular motions have only a small effect on the electronic structure of the crystal. Note that the constant-free-time and constant-free-path approximations are very crude especially for organic molecular crystal systems, because the highly anisotropic crystal environments and somewhat small (compared to traditional inorganic semiconductors) intermolecular interactions contradict the basic assumptions behind these approximations. Early investigations related to bandlike mobility calculations tried to compare the predicted mobility anisotropy to the experimental data in order to verify the theory;[2,23,24] this should be taken with much caution because of the possible differences

TABLE III. Widths of excess electron and hole bands (units: meV).

	Naphthalene		Anthracene		Tetracene		Pentacene	
Direction	HOMO	LUMO	HOMO	LUMO	HOMO	LUMO	HOMO	LUMO
a^{+}[a]	75.65	183.95	249.26	251.44	207.71	275.22	560.89	548.77
a^{-}[b]	87.62	183.95	249.26	251.44	306.76	113.59	173.40	172.16
a_{gap}[c]	0.00	0.00	0.00	0.00	111.02	89.53	4.08	7.08
a_{width}[d]	163.27	367.90	498.52	502.87	625.49	478.34	738.37	728.00
b^{+}	235.65	228.58	442.46	371.17	305.13	225.15	377.76	362.64
b^{-}	103.11	139.32	67.43	131.70	300.77	245.83	355.44	362.64
b_{gap}	0.00	0.00	0.00	0.00	19.59	6.26	5.17	2.72
b_{width}	266.38	367.90	509.89	502.87	625.49	477.24	738.37	728.00
c^{+}	111.57	4.35	88.17	19.05	45.89	57.38	30.09	41.27
c^{-}	99.59	28.30	88.17	37.55	41.54	78.06	7.78	41.27
c_{gap}	163.27	339.60	322.19	446.27	538.06	341.80	700.50	645.47
c_{width}	374.43	372.25	498.52	502.87	625.49	477.24	738.37	728.00
d_1^{+}	229.67	228.58	442.46	371.17	216.50	208.50	523.09	539.88
d_1^{-}	66.40	139.32	56.06	131.70	307.19	93.08	113.28	183.12
$d_{1_{\text{gap}}}$	0.00	0.00	0.00	0.00	101.79	175.66	102.00	5.00
$d_{1_{\text{width}}}$	229.67	367.90	498.52	502.87	625.49	477.24	738.37	728.00
d_2^{+}	229.67	228.58	442.46	371.17	205.12	271.79	542.88	536.89
d_2^{-}	66.40	139.32	56.06	131.70	306.43	93.08	191.58	160.28
$d_{2_{\text{gap}}}$	0.00	0.00	0.00	0.00	101.79	175.66	3.91	30.82
$d_{2_{\text{width}}}$	229.67	367.90	498.52	502.87	625.49	477.24	738.37	728.00
Total[e]	409.00	372.30	509.40	508.30	625.50	502.70	738.40	728.00

[a]Widths of the upper bands.
[b]Widths of the lower bands.
[c]Widths of the gaps between the upper and lower bands.
[d]Total bandwidth along this direction.
[e]3D total bandwidths are calculated from the widths of the continuous region in the DOS spectrum.

of scattering processes along different crystal directions, and considering the band structure effect alone is unlikely to account for the real anisotropy in mobilities.

IV. POLARONIC EFFECTS

In order to understand the temperature dependence of the mobilities, one should include the possibility of the formation of polaron bands.[16] Especially in the case of the oligoacene crystals where low frequency optical modes exist, excitation of these optical modes can change the transfer matrix elements significantly since the transfer matrix elements are strongly dependent on orbital overlap in these systems.[33] In the oligoacene crystals, there are in fact low lying librational modes that will be moderately to strongly coupled to the transfer matrix elements.[35] A theoretical description of the effect of a strongly coupled optical mode on the diffusion or mobility of an electron or hole in a molecular crystal was first given by Holstein[36] and discussed further by many other authors.[16,37–39] Here we will only use the results of these theoretical investigations.

We assume that at least one optical mode is coupled moderately strongly to the transfer matrix elements and that the bandwidth of this mode is much smaller than its frequency, so that we can approximate the optical mode as a local mode. We also assume that the coupling constant of that local mode to the transfer matrix elements is approximately independent of the sites involved in the transfer matrix element. Finally we assume that the coupling is not strong enough to localize the electron or hole, so that the correct description of the transport is that of a polaron band model (i.e., that hopping transport, although described by the

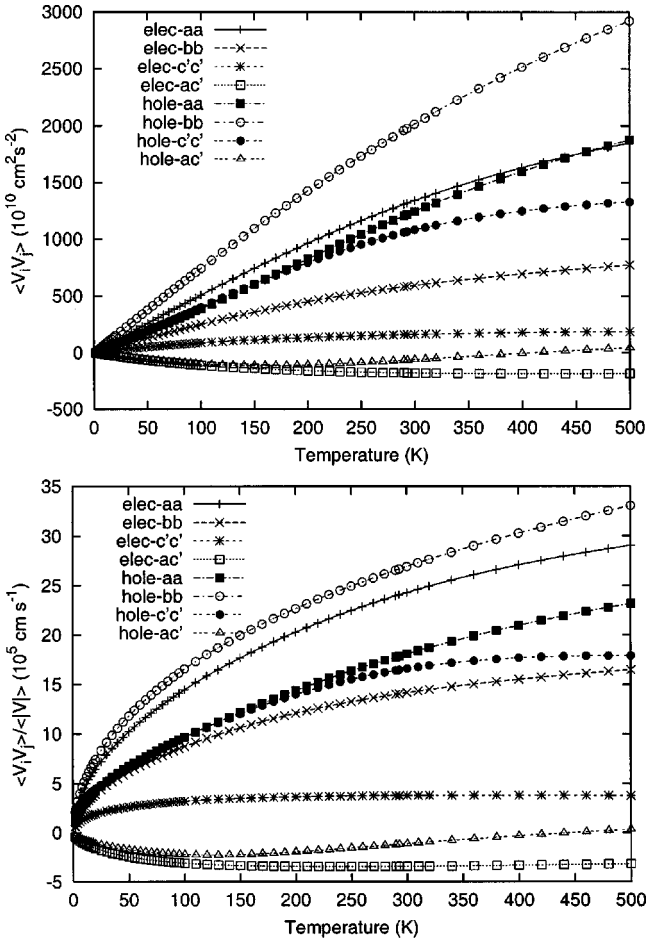

FIG. 5. Temperature dependence of naphthalene velocity–velocity tensor under constant-free-time approximation (upper panel) and constant-free-path approximation (lower panel).

TABLE IV. Components of thermal averaged velocity–velocity tensor product in constant-free-time and constant-free-path approximations at 50 K.

	Naphthalene		Anthracene		Tetracene		Pentacene	
	Hole	Elec.	Hole	Elec.	Hole	Elec.	Hole	Elec.
$\langle V_a^2\rangle^a$	191.19	261.19	376.12	435.62	358.76	556.63	852.48	137.47
$\langle V_b^2\rangle^a$	380.04	131.95	618.32	122.26	537.92	365.56	532.15	528.47
$\langle V_{c'}^2\rangle^a$	199.08	52.88	351.97	158.08	312.27	416.25	251.48	355.19
$\langle V_a V_{c'}\rangle^a$	−57.40	−64.92	−111.80	−58.62	−140.79	−95.96	0.98	−75.27
$\langle V_a V_b\rangle^a$	0	0	0	0	197.94	−48.06	72.68	46.81
$\langle V_b V_{c'}\rangle^a$	0	0	0	0	−134.86	−160.37	−32.92	79.35
$\langle V_a^2/\lvert V\rvert\rangle^b$	6.75	10.21	9.85	13.32	9.56	13.12	17.82	4.72
$\langle V_b^2/\lvert V\rvert\rangle^b$	11.81	6.20	14.57	4.96	13.49	9.54	12.30	13.99
$\langle V_{c'}^2/\lvert V\rvert\rangle^b$	6.72	2.61	9.38	6.25	8.82	10.76	6.93	10.60
$\langle V_a V_{c'}/\lvert V\rvert\rangle^b$	−1.74	−2.46	−2.31	−1.46	−3.22	−2.07	0.01	−1.99
$\langle V_a V_b/\lvert V\rvert\rangle^b$	0	0	0	0	4.29	−0.80	1.55	1.18
$\langle V_b V_{c'}/\lvert V\rvert\rangle^b$	0	0	0	0	−2.81	−3.53	−0.69	−1.79

[a]Constant free-time approximation; units: 10^{10} cm^2 s^{-2}.
[b]Constant free-path approximation; units: 10^5 cm s^{-1}.

same Hamiltonian, is a small term in the temperature range of interest). Under these circumstances, the effect of the electron–optical phonon coupling is to make the effective bandwidth temperature dependent. As the temperature increases, the effective bandwidth decreases.

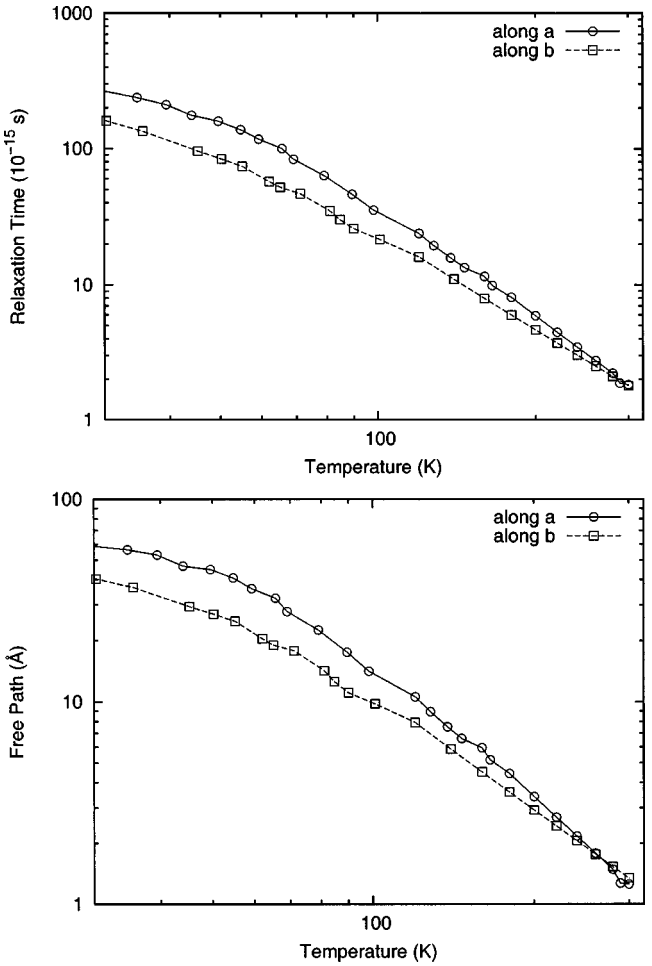

FIG. 6. Temperature dependence of calculated hole relaxation time (upper panel) and hole free path (lower panel) for naphthalene crystal. Results along the crystal **a** direction (open circle) and **b** direction (open square) are presented.

In the small polaron theory, the standard form to describe the temperature dependence of the effective transfer matrix elements is

$$t_{\text{eff}} = \overline{t}\exp(-g^2\coth(\beta\omega/2)), \tag{9}$$

where g is the electron–optical phonon coupling constant, ω is the optical phonon frequency, and β is $1/k_bT$. As a simple test, we use Eq. (9) to calculate the effective transfer matrix elements at different temperatures, and then use the results to construct the polaron band structure and calculate velocity–velocity tensors according to the procedure described in Sec. II. Several different values of both g and ω are used to perform the calculation, and we found that only a large ω and small g can produce a reasonable fit to the experimental power law results. However, the exponential band-narrowing effect described in Eq. (9) results in a exponential decrease of mobility when $k_bT > \omega$, contradicting the power law results observed in experiments. Therefore, a full-dressed small polaron band theory is inadequate for describing the charge-carrier mobilities in oligoacene single crystals. Similar results appear to have been obtained by Giuggioli *et al.* independently to the present work.[40] Given that in organic crystals, the electron–phonon coupling constant is believed to be small to intermediate in value and the bare bandwidth is large, it is possible that the polaron band narrowing effect does not obey a simple exponential form as in Eq. (9). A polaron-band theory that includes the correct band narrowing effect is necessary to adequately describe charge-carrier mobilities in the bandlike regime.

The complicated anisotropic environment as well as the subtle interplay between crystal packing and transfer integrals make the charge-carrier transport in molecular crystals a complicated phenomena. The phonon modes in molecular crystals have different frequency and bandwidth, and also couple to the electronic states with different mechanism and strength. Hence, treating the transport problem with only a single phonon band is unlikely to be adequate. Kenkre *et al.* have used a band model with both acoustic and optical phonon scattering to obtain a reasonable fit to the pentacene experimental data in the band-transportation regime.[41] Here,

we suggest that at least a two-phonon band model, one moderately to strongly coupled and the other weakly coupled, is necessary. The strongly coupled mode (most likely an intermolecular optical mode) *dresses* the carrier and produces a polaron band, and the weakly coupled mode (most likely an acoustic mode) does the scattering among the polaron band states. As a result, the temperature dependence of mobilities is due to both the temperature dependent polaron bandwidth and the temperature dependent scattering rate. The key issue in the success of this model is to obtain the correct form of the polaron band narrowing effect.

V. CONCLUSION

In this paper, transfer integrals for four oligoacene single crystals are calculated using the INDO semiempirical method, and then used to construct the excess electron and hole band structures in the tight-binding approximation. The band structure results suggest that a two-band model is necessary to understand the trend of mobilities in different oligoacene crystals, and the width of the upper HOMO band or the width of the lower LUMO band is a better parameter for estimating the mobility for excess holes or electrons, respectively. Our theoretical model can be used to explain the experimental results that the hole mobility is higher than the electron mobility in oligoacene single crystals and that compounds with a longer conjugation length tend to have higher mobility values.

From these band structures, thermal-averaged velocity–velocity tensors are evaluated using a standard semiconductor band theory. We have compared these tensors to recent experimental data. We conclude that a simple band model is unable to explain the temperature dependence of the charge carrier mobility in oligoacene crystal systems for temperatures higher than 150 K and that the approximations that constant-free-time and constant-free-path are isotropic are open to criticism. In conclusion, a simple wide-band theory is insufficient for describing charge-carrier mobilities of oligoacene single crystals even in the bandlike regime.

A closer study of the polaron effect using the standard small polaron narrowing model shows that a fully-dressed small polaron band theory is also inadequate for describing the charge-carrier mobilities in oligoacene single crystals. This result suggests that the next step beyond the simple band model will be to develop a model that can explicitly include the polaronic effects, i.e., scattering processes between charge carriers and crystal phonons, and further understand the mechanisms of electron–phonon interactions.

ACKNOWLEDGMENTS

The work at MIT has been partly supported by the National Science Foundation (DMR-9808941). The work at Arizona has been partly supported by the National Science Foundation (CHE-0078819), the IBM Shared University Research Program, the Office of Naval Research, and the Petroleum Research Fund. J.C. is a Research Associate of the Belgian National Fund for Scientific Research, FNRS. J.P.C. holds a scholarship from the Belgian FRIA and thanks FNRS for financial support that made his stay at Arizona possible. D.A.F. is supported by the Brazilian agency CAPES.

[1] R. G. Kepler, Phys. Rev. **119**, 1226 (1960).
[2] O. H. LeBlanc, J. Chem. Phys. **35**, 1275 (1961).
[3] M. Pope and C. E. Swenberg, *Electronic Processes in Organic Crystals* (Oxford University Press, New York, 1982).
[4] E. A. Silinsh and V. Čápek, *Organic Molecular Crystals: Interaction, Localization, and Transport Phenomena* (AIP, New York, 1994).
[5] *Organic Electronic Materials: Conjugated Polymers and Low Molecular Weight Organic Solids*, edited by R. Farchioni and G. Grosso (Springer, New York, 2001).
[6] C. D. Dimitrakopoulos and D. J. Mascaro, IBM J. Res. Dev. **45**, 11 (2001).
[7] H. Klauk, D. J. Gundlach, J. A. Nichols, and T. N. Jackson, IEEE Trans. Electron Devices **46**, 1258 (1999).
[8] W. Warta and N. Karl, Phys. Rev. B **32**, 1172 (1985).
[9] D. Gundlach, Y. Lin, T. Jackson, S. Nelson, and D. Schlom, IEEE Electron Device Lett. **18**, 87 (1997).
[10] N. Karl, J. Vac. Sci. Technol. A **17**, 2318 (1999).
[11] N. Karl and J. Marktanner, Mol. Cryst. Liq. Cryst. **355**, 149 (2001).
[12] L. B. Schein, C. B. Duke, and A. R. McGhie, Phys. Rev. Lett. **40**, 197 (1978).
[13] L. Schein, W. Warta, A. R. McGhie, and N. Karl, Chem. Phys. Lett. **100**, 34 (1983).
[14] C. B. Duke, A. Paton, W. R. Salaneck, H. R. Thomas, E. W. Plummer, A. J. Heeger, and A. G. MacDiarmid, Chem. Phys. Lett. **59**, 146 (1978).
[15] J. D. Andersen, C. B. Duke, and V. M. Kenkre, Phys. Rev. Lett. **51**, 2202 (1983).
[16] V. M. Kenkre, J. D. Andersen, D. H. Dunlap, and C. B. Duke, Phys. Rev. Lett. **62**, 1165 (1989).
[17] S. Nelson, Y. Lin, D. Gundlach, and T. Jackson, Appl. Phys. Lett. **72**, 1854 (1998).
[18] N. Karl, *Organic Semiconductors*, Vol. 17 in *Landolt Börnstein/New Series Group III* (Springer, Berlin, 1985), Subvol. 17i, pp. 106–218.
[19] N. Karl, Mol. Cryst. Liq. Cryst. **171**, 31 (1989).
[20] J. Ridley and M. C. Zerner, Theor. Chim. Acta **32**, 111 (1973).
[21] J. Cornil, J. P. Calbert, D. Beljonne, R. Silbey, and J. L. Brédas, Adv. Mater. **12**, 978 (2000).
[22] J. Cornil, J. P. Calbert, and J. L. Brédas, J. Am. Chem. Soc. **123**, 1250 (2001).
[23] J. I. Katz, S. A. Rice, S. il Choi, and J. Jortner, J. Chem. Phys. **39**, 1683 (1963).
[24] R. Silbey, J. Jortner, S. A. Rice, and M. T. Vala, J. Chem. Phys. **42**, 733 (1965).
[25] D. Beljonne, J. Cornil, R. Silbey, P. Millie, and J. L. Bredas, J. Chem. Phys. **112**, 4749 (2000).
[26] V. I. Ponomarev, O. S. Filipenko, and L. O. Atovmyan, Kristallografiya **21**, 392 (1976).
[27] C. P. Brock and J. D. Dunitz, Acta Crystallogr., Sect. B: Struct. Sci. **46**, 795 (1990).
[28] D. Holmes, S. Kumaraswamy, A. J. Matzger, and K. P. C. Vollhardt, Chem.-Eur. J. **5**, 3399 (1999).
[29] M. C. Zerner, G. H. Loew, R. F. Kichner, and U. T. Mueller-Westerhoff, J. Am. Chem. Soc. **107**, 3902 (1980).
[30] R. M. Glaeser and R. S. Berry, J. Chem. Phys. **44**, 3797 (1966).
[31] W. Warta, R. Stehle, and N. Karl, Appl. Phys. A: Solids Surf. **36**, 163 (1985).
[32] N. Karl, J. Cryst. Growth **99**, 1009 (1990).
[33] J. L. Brédas, J. P. Calbert, D. A. da Silva, and J. Cornil, Proc. Natl. Acad. Sci. U.S.A. **99**, 5804 (2002).
[34] R. Haddon, X. Chi, M. Itkis, J. Anthony, D. Eaton, T. Siegrist, C. Mattheus, and T. Palstra, J. Phys. Chem. B **106**, 8288 (2002).
[35] H. Sumi, J. Chem. Phys. **70**, 3775 (1979).
[36] T. Holstein, Ann. Phys. (N.Y.) **8**, 325 (1959).
[37] R. Silbey and R. W. Munn, J. Chem. Phys. **72**, 2763 (1980).
[38] D. R. Yarkony and R. Silbey, J. Chem. Phys. **67**, 5818 (1977).
[39] D. Emin, Adv. Phys. **22**, 57 (1973).
[40] L. Giuggioli, J. D. Andersen, and V. M. Kenkre (preprint).
[41] V. M. Kenkre (private communication).